

# Isolation of Two Different Ni<sub>2</sub>Zn Complexes with an Unprecedented Cocrystal Formed by One of Them and a “Coordination Positional Isomer” of the Other

Lakshmi Kanta Das,<sup>†</sup> Apurba Biswas,<sup>†</sup> Carlos J. Gómez-García,<sup>‡</sup> Michael G. B. Drew,<sup>§</sup> and Ashutosh Ghosh<sup>\*,†</sup>

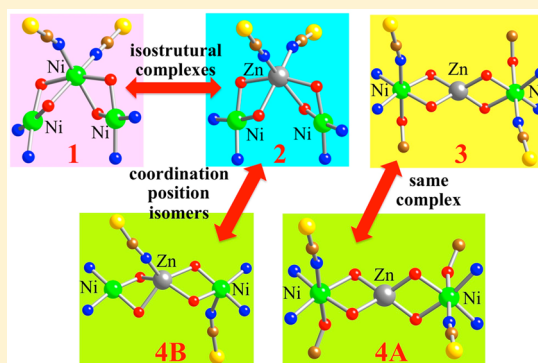
<sup>†</sup>Department of Chemistry, University College of Science, University of Calcutta, 92, APC Road, Kolkata-700009, India

<sup>‡</sup>Instituto de Ciencia Molecular (ICMol), Universidad de Valencia. C/Catedrático José Beltrán, 2, 46980 Paterna, Valencia, Spain

<sup>§</sup>School of Chemistry, The University of Reading, P.O. Box 224, Whiteknights, Reading RG6 6AD, United Kingdom

## Supporting Information

**ABSTRACT:** A new homometallic trinuclear Ni(II) complex [(NiL)<sub>2</sub>Ni(NCS)<sub>2</sub>] (1) and three heterometallic trinuclear Ni(II)–Zn(II)–Ni(II) complexes [(NiL)<sub>2</sub>Zn(NCS)<sub>2</sub>] (2), [(NiL)<sub>2</sub>Zn(NCS)<sub>2</sub>(CH<sub>3</sub>OH)<sub>2</sub>]·2CH<sub>3</sub>OH (3) and {[(NiL)<sub>2</sub>Zn(NCS)<sub>2</sub>(CH<sub>3</sub>OH)<sub>2</sub>]} {[(NiL)<sub>2</sub>Zn(NCS)<sub>2</sub>]} (4) have been synthesized by using the “complex as ligand” approach with the “metalloligand” [NiL] (H<sub>2</sub>L = *N,N'*-bis(salicylidene)-1,3-propanediamine) and thiocyanate in different ratios. All the complexes have been structurally and magnetically characterized. In the isomorphous complexes 1 and 2, the two terminal square planar Ni atoms and the central octahedral nickel atom (in 1) or zinc atom (in 2) are arranged in a bent structure where two *cis*  $\kappa$ N-SCN<sup>−</sup> thiocyanate ions are coordinated to the central atom. The chemical composition of 3 is very similar to that of 2 but, in 3, the central Zn atom is tetrahedral and the  $\kappa$ N-SCN<sup>−</sup> thiocyanate ions occupy an axial position of each terminal nickel atom (which now are octahedral with the sixth position occupied by a methanol molecule). Complex 4 consists of two closely related trinuclear units 4A and 4B. In 4A, the coordination environments of the metals are identical to those of 3 whereas 4B is a “coordination position isomer” of complex 2 with the central square pyramidal Zn and one of the terminal square pyramidal Ni atoms coordinated by two  $\kappa$ N-SCN<sup>−</sup> thiocyanate ions. Complex 4 is a unique example of a cocrystal formed by two similar trinuclear units (4A and 4B) where 4A is identical to an existing complex (3) and 4B is a “coordination position isomer” of another existing complex (2).



## INTRODUCTION

The isolation, identification and characterization of different crystal forms represents one of the most active areas of modern solid state chemistry because these are associated with different solid state phenomena and properties, which are important in both academic and industrial purposes.<sup>1–6</sup> Isomerism and cocrystal formation are fundamental solid state phenomena. Isomerism has been a very important aspect in the development of coordination chemistry.<sup>7</sup> It arises when two or more forms of a complex are found having different structures either in atom connectivity or in the orientation of atoms in space. Various type of isomerism, e.g., ionization, hydrate, linkage,<sup>8</sup> polymerization, coordination, coordination position, valence, geometric (*cis*–*trans*, *fac*–*mer*), optical, etc. have been well recognized since the time of Werner.<sup>9,10</sup> Among these, “coordination position” isomerism is arguably the least familiar as examples are found very rarely.<sup>11</sup> Such isomerism occurs in multinuclear complexes with different arrangements of coordinating groups relative to the metal ions. On the other hand, cocrystals are a subject of great and growing interest in

the study of organic and of pharmaceutical industries.<sup>12–14</sup> They are defined as solids that are crystalline materials composed of two or more different molecular and/or ionic compounds generally in a stoichiometric ratio in the same crystal lattice.<sup>15</sup> If the molecular and/or ionic components within the cocrystal contain similar structures, comparable potential energies and almost similar crystallization kinetics, then cocrystallization is easier.<sup>16</sup> There are many examples of cocrystals of organic molecules,<sup>13,14,17–27</sup> and formation of these species can be explained on the basis of noncovalent interactions. In contrast, cocrystals containing metal complexes are relatively rare<sup>28–33</sup> due to the fact that compounds with different geometries rarely possess similar lattice packing forces and exhibit similar crystallization kinetics.

Recently, we have focused our attention on the synthesis of heterometallic polynuclear complexes based on neutral “metalloligands” (mononuclear Cu(II) or Ni(II) complexes with salen

Received: September 24, 2013

Published: December 18, 2013



type  $N_2O_2$  donor tetradentate di-Schiff base ligands, salen =  $N,N'$ -bis(salicylidene)-ethylenediamine) and some pseudohalides ( $N_3^-$ ,  $NCS^-$ ,  $NCO^-$  and  $N(CN)_2^-$ ).<sup>34–41</sup> On the course of our investigations, we succeeded in isolating several trinuclear molecules with bent and linear shapes and also observed important solid state phenomena such as “polymorphism”<sup>35,36</sup> “supramolecular isomerism”<sup>40</sup> and “linear-bent” isomerism.<sup>41</sup> In most of the trinuclear heterometallic compounds reported so far, the oxygen atoms of two neutral “metalloligands” chelate the central heterometal ion (usually divalent) and its cationic charges are neutralized by either anionic coligands or counteranions. The molecular geometries of the resulting trinuclear compounds depend upon the nature of the anionic coligands. If these anionic coligands bridge two adjacent metal centers, they will produce linear trinuclear compounds,<sup>42–44</sup> whereas, both linear and bent structures may be obtained when the anions are monodentate<sup>45–49</sup> or noncoordinating.<sup>50</sup>

Here we report the structural and magnetic characterization of a homometallic trinuclear Ni(II) complex  $[(NiL)_2Ni(NCS)_2]$  (**1**) and three heterometallic trinuclear Ni(II)–Zn(II)–Ni(II) complexes  $[(NiL)_2Zn(NCS)_2]$  (**2**),  $[(NiL)_2Zn(NCS)_2(CH_3OH)_2] \cdot 2CH_3OH$  (**3**) and  $\{[(NiL)_2Zn(NCS)_2(CH_3OH)_2]\} \{[(NiL)_2Zn(NCS)_2]\}$  (**4**), which are synthesized by the “complex as ligand” strategy with the “metalloligand”  $[NiL]$  (where  $H_2L = N,N'$ -bis(salicylidene)-1,3-propanediamine) and thiocyanate anion. Complexes **1** and **2** are isostructural bent trinuclear species whereas **3** is a linear trinuclear complex, and complex **4** is a cocrystal formed by two linear trinuclear units **4A** and **4B**. The trinuclear unit **4A** is identical to complex **3** and **4B** is a “coordination position isomer” of complex **2**. To the best of our knowledge, complex **4** is the first known example of a dual-component cocrystal formed by trinuclear heterometallic complexes with any Schiff base ligand.

## EXPERIMENTAL SECTION

**Starting Materials.** The salicylaldehyde and 1,3-propanediamine were purchased from Lancaster and were of reagent grade. They were used without further purification.

**Caution!** Perchlorate salts of metal complexes with organic ligands are potentially explosive. Only a small amount of material should be prepared and it should be handled with care.

**Synthesis of the Schiff Base Ligand  $N,N'$ -Bis(salicylidene)-1,3-propanediamine ( $H_2L$ ) and the “Metalloligand”  $[NiL]$ .** The Schiff base ligand was synthesized by standard methods: 5 mmol of 1,3-propanediamine (0.42 mL) was mixed with 10 mmol of salicylaldehyde (1.04 mL) in methanol (20 mL). The resulting solution was refluxed for ca. 2 h and was allowed to cool. The yellow methanolic solution was used directly for complex formation. An aqueous solution (20 mL) of  $Ni(ClO_4)_2 \cdot 6H_2O$  (1.820 g, 5 mmol) and 10 mL of ammonia solution (20%) were added to a methanolic solution of  $H_2L$  (10 mL, 5 mmol) to prepare the “metalloligand”  $[NiL]$ , as reported earlier.<sup>51</sup>

**Synthesis of  $[(NiL)_2Ni(NCS)_2]$  (**1**) and  $[(NiL)_2Zn(NCS)_2]$  (**2**).** The previously prepared  $[NiL]$  complex (0.642 g, 2 mmol) was dissolved in methanol (20 mL) and then an aqueous solution (1 mL) of  $Ni(ClO_4)_2 \cdot 6H_2O$  (0.364 g, 1 mmol), and an aqueous solution (1 mL) of ammonium thiocyanate (0.152 g, 2 mmol) were added. The mixture was stirred for 1 h at room temperature when a red solid separated out. The solid was filtered, and the filtrate was allowed to stand overnight, resulting in the formation of prismatic red X-ray quality single crystals of **1**. The brown rhombic-shaped single crystals of complex **2** were obtained in the same manner as **1**, except that  $Zn(ClO_4)_2 \cdot 6H_2O$  (0.372 g, 1 mmol) was used in the synthesis instead of  $Ni(ClO_4)_2 \cdot 6H_2O$ . Both compounds were washed with diethyl ether and dried in a desiccator containing anhydrous  $CaCl_2$ .

**Complex 1.** Yield: 0.705 g (83%). Anal. Calcd for  $C_{36}H_{32}Ni_3N_6O_4S_2$ : C 50.70, H 3.78, N 9.85%. Found: C 50.59, H 3.87, N 9.88%. UV/vis:  $\lambda_{max}$  ( $CH_3OH$ ) = 592, 407 and 343 nm;  $\lambda_{max}$  (solid, reflectance) = 630, 510 and 391. IR (KBr):  $\nu$  (C=N) 1610 and  $\nu$  (SCN) 2085  $cm^{-1}$ .

**Complex 2.** Yield: 0.650 g (76%). Anal. Calcd for  $C_{36}H_{32}Ni_2N_6O_4S_2Zn$ : C 50.30, H 3.75, N 9.78%. Found: C 50.41, H 3.55, N 9.71%. Ni:Zn ratio = 66.2:33.8 (determined by electron probe micro analysis). UV/vis:  $\lambda_{max}$  ( $CH_3OH$ ) = 590, 405 and 337 nm;  $\lambda_{max}$  (solid, reflectance) = 624, 499 and 390. IR (KBr):  $\nu$  (C=N) 1625 and  $\nu$  (SCN) 2088  $cm^{-1}$ . HRMS ( $m/z$ , ESI<sup>+</sup>): found for  $[(NiL)H]^+$  = 339.08 (calcd 339.06),  $[(NiL)Na]^+$  = 361.10 (calcd 361.05),  $[(NiL)_2H]^+$  = 677.11 (calcd 677.12),  $[(NiL)_2Na]^+$  = 699.11 (calcd 699.10).

**Synthesis of  $[(NiL)_2Zn(NCS)_2(CH_3OH)_2] \cdot 2CH_3OH$  (**3**).** Complex **3** was prepared by mixing the same components as for **2** but with different stoichiometric ratios. The precursor “metalloligand”  $[NiL]$  (1.284 g, 4 mmol) was dissolved in methanol (20 mL) and then an aqueous solution (1 mL) of  $Zn(ClO_4)_2 \cdot 6H_2O$  (0.373 g, 1 mmol), and an aqueous solution (1 mL) of ammonium thiocyanate (0.152 g, 2 mmol) were added to this solution. The solution was stirred for 1 h at room temperature. In this case, a small amount of light blue product separated out upon stirring the solution. The blue rhombic shaped X-ray quality single crystals of **3** were obtained by slow evaporation of the filtrate. The compound was washed with diethyl ether and dried in a desiccator containing anhydrous  $CaCl_2$ .

**Complex 3:** Yield: 0.618 g (63%, calculated with respect to  $Zn(ClO_4)_2 \cdot 6H_2O$ ). Anal. Calcd for  $C_{40}H_{48}Ni_2N_6O_8S_2Zn$ : C 48.64, H 4.90, N 8.51%. Found: C 48.69, H 4.78, N 8.48%. Ni:Zn ratio = 64.2:35.8 (determined by electron probe micro analysis). UV/vis:  $\lambda_{max}$  ( $CH_3OH$ ) = 588, 405 and 337;  $\lambda_{max}$  (solid, reflectance) = 1023, 576, 410 and 364 nm. IR (KBr):  $\nu$  (C=N) 1626 and  $\nu$  (SCN) 2093  $cm^{-1}$ . HRMS ( $m/z$ , ESI<sup>+</sup>): found for  $[(NiL)H]^+$  = 339.05 (calcd 339.06),  $[(NiL)Na]^+$  = 361.04 (calcd 361.05),  $[(NiL)_2H]^+$  = 677.12 (calcd 677.12),  $[(NiL)_2Na]^+$  = 699.06 (calcd 699.10).

**Synthesis of  $\{[(NiL)_2Zn(NCS)_2(CH_3OH)_2]\} \{[(NiL)_2Zn(NCS)_2]\}$  (**4**).** Complex **4** was also prepared by mixing the same components as for **2** and **3** but with a smaller proportion of “metalloligand”. The precursor “metalloligand”  $[NiL]$  (0.321 g, 1 mmol) was dissolved in methanol (20 mL) and then an aqueous solution (1 mL) of  $Zn(ClO_4)_2 \cdot 6H_2O$  (0.373 g, 1 mmol), and an aqueous solution (1 mL) of ammonium thiocyanate (0.152 g, 2 mmol) were added to this solution. The solution was stirred for 1 h at room temperature. Here a red solid product was separated out. The microcrystalline red product was separated by filtration. Evaporation at room temperature of the filtrate yielded red needle shaped X-ray quality single crystals of **4**. The compound was washed with diethyl ether and dried in a desiccator containing anhydrous  $CaCl_2$ .

**Complex 4.** Yield: 0.353 g (58%, calculated with respect to  $[NiL]$ ). Anal. Calcd for  $C_{74}H_{72}Ni_4N_{12}O_{12}S_4Zn_2$ : C 48.96, H 4.00, N 9.26%. Found: C 48.78, H 3.92, N 9.19%. Ni:Zn ratio = 61.1:38.9 (determined by electron probe micro analysis). UV/vis:  $\lambda_{max}$  (MeOH) = 587, 406 and 338 nm;  $\lambda_{max}$  (solid, reflectance) = 1032, 623, 530 and 371 nm. IR (KBr):  $\nu$  (C=N) 1627 and  $\nu$  (SCN) 2075  $cm^{-1}$ . HRMS ( $m/z$ , ESI<sup>+</sup>): found for  $[(NiL)H]^+$  = 339.09 (calcd 339.06),  $[(NiL)Na]^+$  = 361.04 (calcd 361.05),  $[(NiL)_2H]^+$  = 677.13 (calcd 677.12),  $[(NiL)_2Na]^+$  = 699.06 (calcd 699.10).

**Physical Measurements.** Elemental analyses (C, H and N) were performed using a Perkin-Elmer 2400 series II CHN analyzer. IR spectra in KBr pellets (4000–500  $cm^{-1}$ ) were recorded using a Perkin-Elmer RXI FT-IR spectrophotometer. Electronic spectra in methanol and in solid state were recorded in a Hitachi U-3501 spectrophotometer. Powder X-ray diffraction patterns were recorded on a Bruker D-8 Advance diffractometer operated at 40 kV voltage and 40 mA current and calibrated with a standard silicon sample, using Ni-filtered  $Cu K\alpha$  ( $\lambda = 0.15406$  nm) radiation. The electrospray ionization mass spectrometry (ESI-MS positive) spectra were recorded with a Micromass Qtof YA 263 mass spectrometer. The results have been described in the Supporting Information (Figures S1–S3). The Zn and Ni contents and ratios were measured on a Philips ESEM X230

Table 1. Crystal Data and Structure Refinement of Complexes 1–4

complexes	1	2	3	4
formula	C <sub>36</sub> H <sub>32</sub> Ni <sub>3</sub> N <sub>6</sub> O <sub>4</sub> S <sub>2</sub>	C <sub>36</sub> H <sub>32</sub> Ni <sub>2</sub> N <sub>6</sub> O <sub>4</sub> S <sub>2</sub> Zn	C <sub>40</sub> H <sub>48</sub> Ni <sub>2</sub> N <sub>6</sub> O <sub>8</sub> S <sub>2</sub> Zn	C <sub>74</sub> H <sub>72</sub> Ni <sub>4</sub> N <sub>12</sub> O <sub>12</sub> S <sub>4</sub> Zn <sub>2</sub>
<i>M</i>	852.89	859.59	987.75	1815.26
crystal system	monoclinic	monoclinic	monoclinic	monoclinic
space group	<i>P</i> 2 <sub>1</sub> / <i>c</i>	<i>P</i> 2 <sub>1</sub> / <i>c</i>	<i>P</i> 2 <sub>1</sub> / <i>c</i>	<i>C</i> 2/ <i>c</i>
<i>a</i> , Å	12.557(5)	12.598(5)	12.162(5)	27.683(5)
<i>b</i> , Å	9.989(5)	9.960(5)	16.153(5)	9.304(5)
<i>c</i> , Å	28.118(5)	28.247(5)	22.493(5)	30.671(5)
$\beta$ , deg	100.490(5)	101.299(5)	94.635(5)	95.513(5)
<i>V</i> , Å <sup>3</sup>	3468(2)	3476(2)	4404(2)	7863(5)
<i>Z</i>	4	4	4	4
<i>D</i> <sub>o</sub> g cm <sup>-3</sup>	1.633	1.643	1.490	1.533
$\mu$ , mm <sup>-1</sup>	1.783	1.927	1.538	1.712
<i>F</i> (000)	1752	1760	2048	3728
<i>R</i> (int)	0.073	0.075	0.074	0.101
total reflections	39557	35550	27829	46452
unique reflections	6391	7159	7808	9561
<i>I</i> > 2 $\sigma$ ( <i>I</i> )	4427	5399	5166	5287
<i>R</i> 1 <sup>a</sup> , <i>wR</i> 2 <sup>b</sup> For <i>I</i> > 2 $\sigma$ ( <i>I</i> )	0.0405, 0.0856	0.0670, 0.1767	0.0717, 0.1980	0.0596, 0.1832
GOF <sup>c</sup> on <i>F</i> <sup>2</sup>	0.919	1.06	1.04	1.03

$$^a R1 = \sum \|F_o\| - \|F_c\| / \sum \|F_o\| \quad ^b wR2 (F_o^2) = \sum [w(F_o^2 - F_c^2)^2 / \sum wF_o^4]^{1/2} \quad ^c GOF = \sum [w(F_o^2 - F_c^2)^2 / (N_{obs} - N_{params})]^{1/2}$$

scanning electron microscope equipped with an EDAX DX-4 microsonde. Variable temperature magnetic susceptibility measurements were carried out in the temperature range 2–300 K with an applied magnetic field of 0.1 T on polycrystalline samples of complexes **1**, **3** and **4** (with masses of 23.33, 43.61, and 27.89 mg, respectively) with a Quantum Design MPMS-XL-5 SQUID magnetometer. The susceptibility data were corrected for the sample holders previously measured using the same conditions and for the diamagnetic contributions of the salt as deduced by using Pascal's constant tables ( $\chi_{\text{dia}} = -427.58 \times 10^{-6}$ ,  $-519.86 \times 10^{-6}$  and  $-938.58 \times 10^{-6}$  emu·mol<sup>-1</sup> for **1**, **3** and **4**, respectively).<sup>52</sup>

**Crystallographic Data Collection and Refinement.** Well-formed single crystals of each complex were mounted on a Bruker-AXS SMART APEX II diffractometer equipped with a graphite monochromator and Mo *K* $\alpha$  ( $\lambda = 0.71073$  Å) radiation. The crystals were positioned 60 mm from the CCD, and frames (360) were measured with a counting time of 5 s at 293 K. The structures were solved using the Patterson method through the SHELXS 97 program, while difference Fourier synthesis and least-squares refinement confirmed the positions of the non-hydrogen atoms, which were refined with anisotropic displacement parameters. Hydrogen atoms were placed in idealized positions and their displacement parameters were fixed to be 1.2 times larger than those of the atom to which they were attached. Absorption corrections were carried out using the SADABS program,<sup>53</sup> while all calculations were made via SHELXS 97,<sup>54</sup> SHELXL 97,<sup>55</sup> PLATON 99,<sup>56</sup> ORTEP-32<sup>57</sup> and WINGX system ver-1.64.<sup>58</sup> Data collection, structure refinement parameters and crystallographic data for the four complexes are given in Table 1.

In unit **4B**, the two Ni(II) atoms are equivalent due to the presence of a *C*<sub>2</sub> axis but there is only one  $\kappa N$ -SCN<sup>-</sup> ligand coordinated to the Ni(II) ions. Accordingly, we found a disorder with an occupancy factor of 1/2 for this  $\kappa N$ -SCN<sup>-</sup> ligand coordinated to the Ni(II) ions. This disorder implies that the  $\kappa N$ -SCN<sup>-</sup> ligand is coordinated to one Ni(II) ion in one-half of the **4B** units and to the other Ni(II) ion in the other half.

## RESULTS AND DISCUSSION

**Syntheses of the Complexes.** The Schiff-base ligand (H<sub>2</sub>L) and its Ni(II) complex, [NiL], were synthesized using the reported procedure.<sup>51</sup> The Ni(II) complex, on reaction with nickel perchlorate hexahydrate and ammonium thiocyanate in a 2:1:2 molar ratio at room temperature, resulted in the trinuclear

Ni(II) complex [(NiL)<sub>2</sub>Ni(NCS)<sub>2</sub>] (**1**). The microcrystalline red product, which is isolated on stirring, is pure **1**, as its powder XRD pattern is identical to that simulated from the X-ray structure of **1** (Figure S4, Supporting Information). The prismatic red single crystals of **1** were obtained on keeping the filtrate overnight in the open atmosphere. Interestingly, a reaction of the same “metalloligand” [NiL] and ammonium thiocyanate with zinc perchlorate, instead of nickel perchlorate, at room temperature, resulted in three different heterometallic complexes: [(NiL)<sub>2</sub>Zn(NCS)<sub>2</sub>] (**2**), [(NiL)<sub>2</sub>Zn(NCS)<sub>2</sub>(CH<sub>3</sub>OH)<sub>2</sub>]·2CH<sub>3</sub>OH (**3**) and {[(NiL)<sub>2</sub>Zn(NCS)<sub>2</sub>(CH<sub>3</sub>OH)<sub>2</sub>]} {[(NiL)<sub>2</sub>Zn(NCS)<sub>2</sub>]} (**4**), depending on the molar ratios of the reactants. When [NiL], Zn(II) and SCN<sup>-</sup> were mixed in the same stoichiometric ratio as for **1** i.e., in 2:1:2 molar ratio, then a brown microcrystalline product of complex **2** was obtained. A comparison of the powder XRD patterns of this brown product with that of the simulated powder XRD pattern of the single crystal (Figure S4, Supporting Information) clearly showed that it is pure **2**. Complex **2** crystallizes as brown rhombic-shaped single crystals. Complex **3** was synthesized by using the same components but with an increase in the proportion of “metalloligand” [NiL] i.e., mixing [NiL], Zn(II) and SCN<sup>-</sup> in a 4:1:2 molar ratio. The powder XRD pattern of the isolated light blue microcrystalline product is identical to that obtained from simulation of the crystal data of **3**, indicating its phase purity (Figure S4, Supporting Information). Complex **3** crystallizes as blue rhombic-shaped single crystals. Finally, when [NiL], Zn(II) and SCN<sup>-</sup> were mixed in a 1:1:2 molar ratio at room temperature, i.e., decreasing the proportion of “metalloligand” [NiL], a red solid was isolated from the reaction mixture. The isolated red product is pure **4**, as is evident from its powder XRD pattern (Figure S4, Supporting Information). Red needle-shaped X-ray quality single crystals of **4** were obtained by the slow evaporation of the filtrate in open atmosphere. It is important to mention that although we tried to prepare equivalent Ni(II) complexes, the color and the powder XRD pattern are unchanged when nickel perchlorate hexahydrate and ammonium thiocyanate were mixed in either increasing or

Scheme 1. Formation of Complexes 1–4 and the Transformation of Complexes 4 and 3 to 2

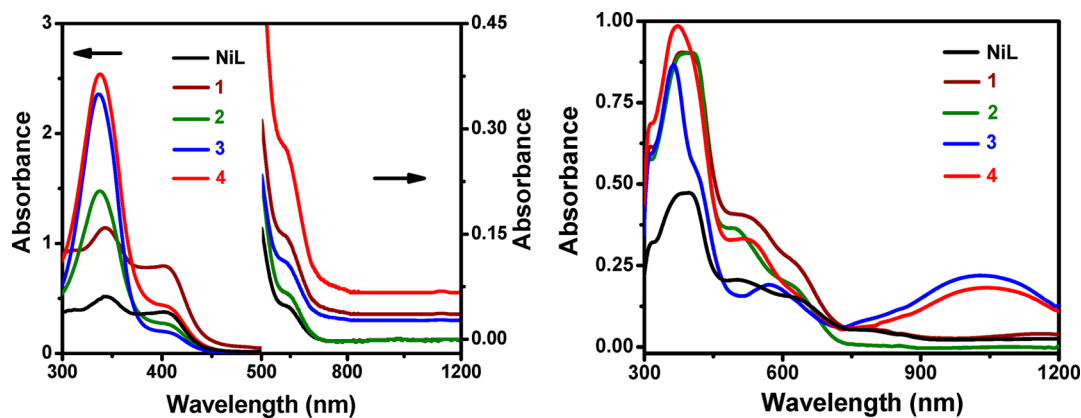
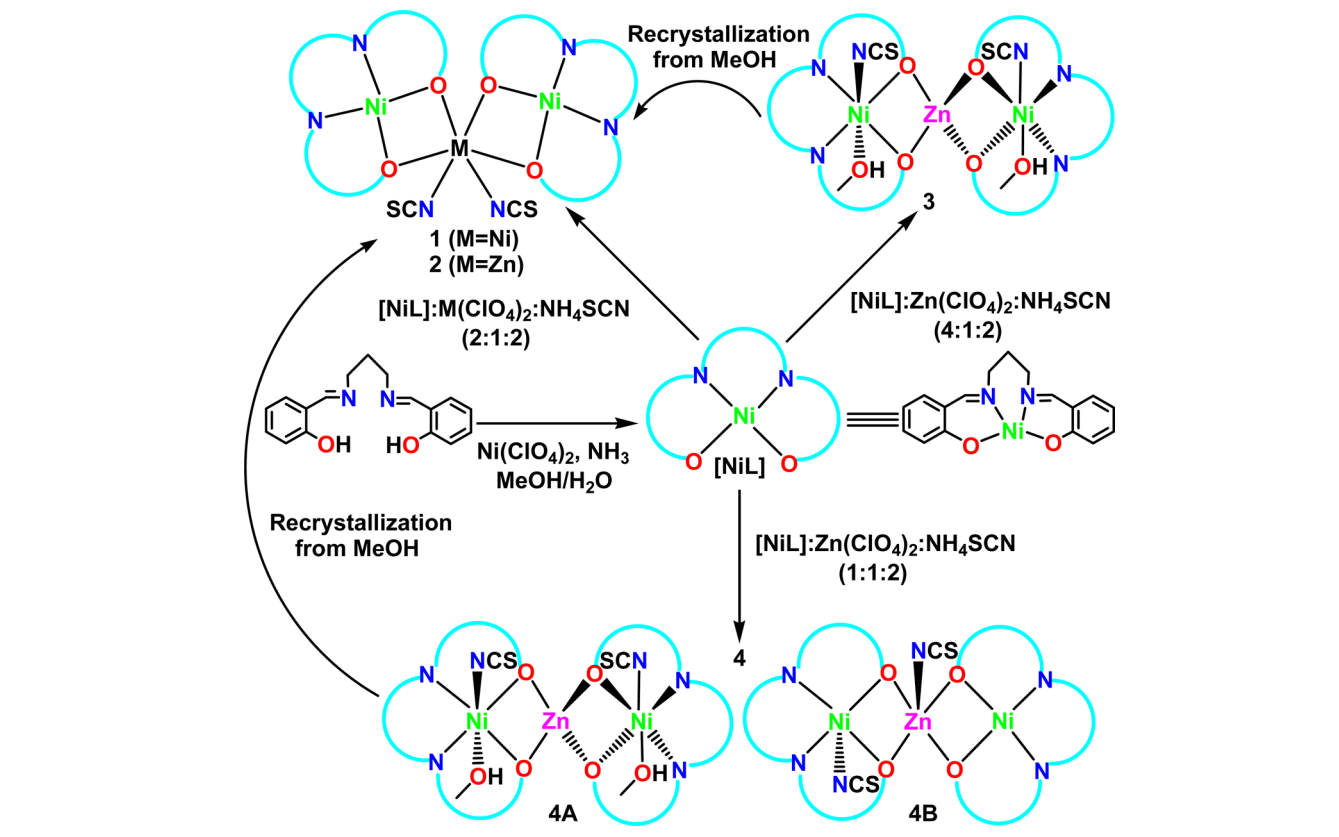


Figure 1. Electronic spectra of the complexes in MeOH (left) and solid state (right).

decreasing proportions of [NiL], thus 1 is the only complex that was obtained with Ni(II). In summary, we can easily obtain complexes 4, 2 and 3 by simply increasing the [NiL] ratio, from 1 to 2 and 4, respectively (fixing the Zn(II):NCS<sup>-</sup> ratio to 1:2, Scheme 1).

It should be noted that both complexes 3 and 4 are transformed to 2 when these are dissolved in methanol separately and the solutions are kept at room temperature for slow evaporation. On the other hand, complexes 1 and 2 do not change to any other form upon recrystallization.

**IR and UV-vis Spectra of the Complexes.** Besides elemental analysis, all the complexes were initially characterized by IR spectra. Like the precursor “metalloligand” [NiL], a strong and sharp band due to the azomethine  $\nu$  (C=N) group of the Schiff base appears at 1610, 1625, 1626 and 1627  $\text{cm}^{-1}$  for complexes 1–4, respectively. The precursor “metalloligand”

[NiL] is neutral and obviously is not associated with any counteranion. Therefore, the characteristic peaks for thiocyanate in the region of 2100–2050  $\text{cm}^{-1}$  indicate the formation of the complexes. These peaks were clearly detected at 2085, 2088, 2093 and 2075  $\text{cm}^{-1}$  in the IR spectra of 1–4, respectively (Figures S5–S8, Supporting Information).

The UV-vis spectra of the complexes in methanolic solution and their solid state diffuse reflectance spectra are shown in Figure 1 and the spectral parameters are given in Table 2. The electronic spectra of all the complexes in methanol are almost identical, but they differ appreciably in the solid state, especially in the visible region. Thus, they show a sharp single absorption band near 343, 337, 337 and 338 nm in methanol and 391, 390, 364 and 371 nm in the solid state for 1–4, respectively, attributed to ligand-to-metal charge transfer transitions. Besides this band, a broad absorption band ( $\nu_1$ ) is observed in the

**Table 2.** UV–Vis Spectral Parameters of the “Metalloligand” and Complexes 1–4

complex	$\lambda_{\max}$ (nm) ( $\epsilon$ , $M^{-1} \text{ cm}^{-1}$ ) in $\text{CH}_3\text{OH}$	$\lambda_{\max}$ (nm) in solid state
[NiL]	592(48), 406(3725) and 343(5227)	387, 508 and 632
1	592 (148), 407(7857) and 343 (11599)	391, 510 and 630
2	590 (70), 405(2775) and 337 (14724)	390, 499 and 624
3	588 (108), 405(1988) and 337 (23555)	364, 410, 576 and 1023
4	587(272), 406(4277) and 338 (25588)	371, 530, 623 and 1032

visible region at 592, 590, 588 and 587 nm along with a less intense shoulder ( $\nu_2$ ) at 407, 405, 405 and 406 nm in methanol for 1–4, respectively, whereas the “metalloligand” [NiL] shows band maxima ( $\nu_1$ ) at 592 nm along with a less intense shoulder ( $\nu_2$ ) at 406 nm. This band is typical of d–d transitions of Ni(II) ions with a square planar environment. The electronic spectrum for a four coordinate nickel(II) compound with a square planar geometry is expected to exhibit absorption bands near 610 ( $\nu_1$ ) and 500 nm ( $\nu_2$ ), corresponding to the spin allowed d–d transitions  ${}^1B_{1g} \leftarrow {}^1A_g$  and  ${}^1B_{3g} \leftarrow {}^1A_g$ , respectively.<sup>59,60</sup> The observation of the  $\nu_1$  and  $\nu_2$  bands confirms the square planar environment around Ni(II) in methanol solutions. However, in the solid state, the band positions of 1 (broad band at 630 nm ( $\nu_1$ ) along with a hump 510 nm ( $\nu_2$ )) and 2 (broad band at 624 nm ( $\nu_1$ ) along with a hump 499 nm ( $\nu_2$ )) are almost the same as in the mononuclear precursor [NiL] (broad band at 623 nm ( $\nu_1$ ) along with a hump 500 nm ( $\nu_2$ )), in agreement with the square planar geometry around Ni(II). On the other hand, 3 exhibits two distinct bands at 576 and 1023 nm, which can be assigned to the spin-allowed d–d transitions  ${}^3T_{1g}(F) \leftarrow {}^3A_{2g}$  and  ${}^3T_{2g} \leftarrow {}^3A_{2g}$ , respectively. These values agree with the literature values for octahedral Ni(II) compounds.<sup>61,62</sup> Moreover, complex 4 shows a weak broad band at 623 nm ( $\nu_1$ ) along with a hump at 530 nm ( $\nu_2$ ) and another well-separated broad band at 1032 nm. The former two bands ( $\nu_1$  and  $\nu_2$ ) are due to the spin allowed d–d transitions  ${}^1B_{1g} \leftarrow {}^1A_g$  and  ${}^1B_{3g} \leftarrow {}^1A_g$  for square planar Ni(II) and the latter band is assignable to the transition  ${}^3T_{2g} \leftarrow {}^3A_{2g}$  for octahedral Ni(II) geometry, in agreement with the structural data (see below).

**Structures of the Complexes.** The structure of 1 is shown in Figure 2 (left) together with the atomic numbering scheme in the coordination spheres. Bond lengths and angles in the metal coordination sphere are given in Table 3. The molecular structure of 1 consists of a neutral trinuclear entity of formula

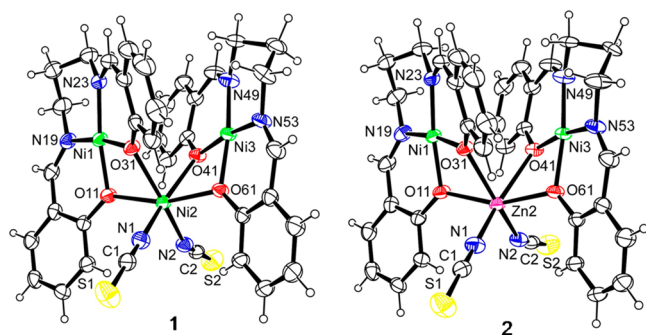


**Figure 2.** Structures of complexes 1 (left) and 2 (right) with ellipsoids at 30% probability. In both structures, the six-membered saturated chelate ring containing atoms N49 and N53 is disordered and two positions were refined for the three methylene groups. Only one possible orientation is shown.

$[(\text{NiL})_2\text{Ni}(\text{NCS})_2]$  (where  $\text{H}_2\text{L} = N,N'$ -bis(salicylidene)-1,3-propanediamine). The structure contains a nickel(II) ion (Ni2) in a distorted octahedral environment together with two square planar nickel(II) ions (Ni1 and Ni3) with similar environments. The two square planar nickel atoms are bonded to two nitrogen atoms and two oxygen atoms from the tetradentate Schiff base ligand with very similar bond lengths (Table 3). The four donor atoms in the equatorial plane show root-mean-squared deviations of 0.053 and 0.028 Å for Ni1 and Ni3, respectively, with the nickel atoms at 0.011(1), 0.021(1) Å from the appropriate mean plane. The trans angles are all close to  $170^\circ$  (Table 3), indicating a slight tetrahedral distortion from the ideal square planar geometry, as confirmed by the low  $\tau_4$  indexes<sup>63</sup> (0.134 for Ni1 and 0.133 for Ni3;  $\tau_4$  is defined as  $\tau_4 = [360^\circ - (\alpha + \beta)]/141^\circ$ , with  $\alpha$  and  $\beta$  (in deg) being the two largest angles around the central metal in the complex with  $\tau_4 = 0$  for a perfect square planar and  $\tau_4 = 1$  for a perfect tetrahedron. The dihedral angle between the two  $\text{N}_2\text{–Ni–O}_2$  planes is  $22.1(1)^\circ$ , indicating that the two “metalloligands” are almost parallel to each other.

The central Ni2 atom has an octahedral environment formed by four oxygen atoms from the two chelating “metalloligands” and by two terminal *cis*  $\kappa\text{N-SCN}^-$  ligands. The geometry is very distorted, primarily due to the small bite angles of the chelating [NiL] metalloligands (ca.  $67\text{--}69^\circ$ ). Interestingly, the two  $\kappa\text{N-SCN}^-$  ligands present different orientations as reflected by their Ni–N–C bond angles [Ni2–N1–C1 =  $176.9(3)^\circ$  and Ni2–N2–C2 =  $150.2(4)^\circ$ ]. The Ni1⋯Ni2, Ni2⋯Ni3 and Ni3⋯Ni1 distances are 3.046(1), 3.045(1) and 4.357(2) Å, respectively. The Ni1–Ni2–Ni3 angle is  $91.33(3)^\circ$ , indicating a nearly perpendicular arrangement of the metal atoms in the bent Ni<sub>3</sub> unit.

Complex 2 is isostructural to 1 but with a central Zn(II) ion, instead of a Ni(II) one, bridging the external square planar Ni(II) atoms (Figure 2; right), thus forming a neutral trinuclear unit of formula  $[(\text{NiL})_2\text{Zn}(\text{NCS})_2]$ . As expected, a comparison of the bond lengths and angles between 1 and 2 shows very small differences (Table 3). Again, there is a small tetrahedral distortion in the equatorial planes around nickel with root-mean-squared deviations of the coordinating atoms of 0.032 and 0.034 Å around Ni1 and Ni3, respectively. The metal atoms are 0.011(31) and 0.024(3) Å from the planes. The  $\tau_4$  values (0.130 for Ni1 and 0.136 for Ni3) also confirm a slightly distorted square planar geometry around the metal centers. The two “metalloligands” are also nearly parallel to each other, as indicated by the dihedral angle ( $20.2(2)^\circ$ ) between the two  $\text{N}_2\text{–Ni–O}_2$  planes.

The zinc atom, Zn(2) has a similar distorted octahedral environment to Ni(2) in complex 1. The *cis* [ $64.5(2)\text{--}104.7(2)^\circ$ ] and *trans* [ $153.9(2)\text{--}158.7(2)^\circ$ ] angles also indicate significant distortions from the ideal octahedral geometry around the zinc atom. The orientation of the two  $\kappa\text{N-SCN}^-$  ligands are also different (Zn2–N1–C1 =  $177.3(6)^\circ$  and Zn2–N2–C2 =  $150.7(5)^\circ$ ). The Zn⋯Ni distances are 3.124(2) and 3.142(2) Å whereas the Ni⋯Ni distance is 4.424(3) Å. Like in 1, the Ni1–Zn2–Ni3 angle ( $89.80(3)^\circ$ ) indicates a nearly perpendicular arrangement of the three metal atoms in the Ni<sub>2</sub>Zn unit.

The noncovalent interactions present between the two trinuclear units in complexes 1 and 2 are also very similar (see Figures S9 and S10, Supporting Information).

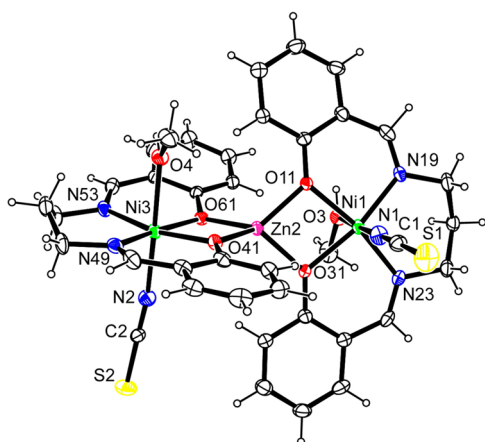
The structure of 3 is shown in Figure 3 together with the atomic numbering scheme. Bond lengths and angles in the

Table 3. Bond Distances (Å) and Angles (deg) for Complexes 1–3

complex 1		complex 2		complex 3	
Ni(1)–O(11)	1.873(3)	Ni(1)–O(11)	1.866(4)	Ni(1)–O(3)	2.181(5)
Ni(1)–O(31)	1.871(3)	Ni(1)–O(31)	1.866(4)	Ni(1)–O(11)	2.044(5)
Ni(1)–N(19)	1.901(4)	Ni(1)–N(19)	1.902(5)	Ni(1)–O(31)	2.047(5)
Ni(1)–N(23)	1.894(4)	Ni(1)–N(23)	1.900(5)	Ni(1)–N(1)	2.048(7)
Ni(2)–O(11)	2.063(3)	Zn(2)–O(11)	2.116(4)	Ni(1)–N(19)	2.022(6)
Ni(2)–O(31)	2.125(3)	Zn(2)–O(31)	2.189(4)	Ni(1)–N(23)	2.024(6)
Ni(2)–O(41)	2.185(3)	Zn(2)–O(41)	2.320(4)	Zn(2)–O(11)	1.954(5)
Ni(2)–O(61)	2.049(2)	Zn(2)–O(61)	2.094(4)	Zn(2)–O(31)	1.947(5)
Ni(2)–N(1)	1.994(4)	Zn(2)–N(1)	2.004(6)	Zn(2)–O(41)	1.952(5)
Ni(2)–N(2)	2.025(4)	Zn(2)–N(2)	2.035(6)	Zn(2)–O(61)	1.956(5)
Ni(3)–O(41)	1.885(3)	Ni(3)–O(41)	1.876(4)	Ni(3)–O(4)	2.204(6)
Ni(3)–O(61)	1.866(3)	Ni(3)–O(61)	1.866(4)	Ni(3)–O(41)	2.053(5)
Ni(3)–N(49)	1.883(3)	Ni(3)–N(49)	1.883(5)	Ni(3)–O(61)	2.046(5)
Ni(3)–N(53)	1.905(3)	Ni(3)–N(53)	1.915(5)	Ni(3)–N(2)	2.043(7)
O(11)–Ni(1)–O(31)	79.16(11)	O(11)–Ni(1)–O(31)	79.0(2)	Ni(3)–N(49)	2.034(7)
O(11)–Ni(1)–N(19)	91.56(13)	O(11)–Ni(1)–N(19)	92.0(2)	Ni(3)–N(53)	2.032(7)
O(11)–Ni(1)–N(23)	170.75(13)	O(11)–Ni(1)–N(23)	171.1(2)	O(3)–Ni(1)–O(11)	87.3(2)
O(31)–Ni(1)–N(19)	170.29(13)	O(31)–Ni(1)–N(19)	170.8(2)	O(3)–Ni(1)–O(31)	87.0(2)
O(31)–Ni(1)–N(23)	92.55(13)	O(31)–Ni(1)–N(23)	92.5(2)	O(3)–Ni(1)–N(1)	179.2(3)
N(19)–Ni(1)–N(23)	96.91(15)	N(19)–Ni(1)–N(23)	96.6(2)	O(3)–Ni(1)–N(19)	85.6(2)
O(11)–Ni(2)–O(31)	69.41(11)	O(11)–Zn(2)–O(31)	66.9(2)	O(3)–Ni(1)–N(23)	90.7(2)
O(11)–Ni(2)–O(41)	99.08(10)	O(11)–Zn(2)–O(41)	98.3(2)	O(11)–Ni(1)–O(31)	79.0(2)
O(11)–Ni(2)–O(61)	162.91(11)	O(11)–Zn(2)–O(61)	158.7(2)	O(11)–Ni(1)–N(1)	92.3(2)
O(11)–Ni(2)–N(1)	95.42(12)	O(11)–Zn(2)–N(1)	97.5(2)	O(11)–Ni(1)–N(19)	90.5(2)
O(11)–Ni(2)–N(2)	94.98(12)	O(11)–Zn(2)–N(2)	94.3(2)	O(11)–Ni(1)–N(23)	168.8(2)
O(31)–Ni(2)–O(41)	79.56(10)	O(31)–Zn(2)–O(41)	76.1(2)	O(31)–Ni(1)–N(1)	93.6(3)
O(31)–Ni(2)–O(61)	96.68(10)	O(31)–Zn(2)–O(61)	95.5(2)	O(31)–Ni(1)–N(19)	167.4(2)
O(31)–Ni(2)–N(1)	94.35(14)	O(31)–Zn(2)–N(1)	96.0(2)	O(31)–Ni(1)–N(23)	89.9(2)
O(31)–Ni(2)–N(2)	159.67(13)	O(31)–Zn(2)–N(2)	153.9(2)	N(1)–Ni(1)–N(19)	93.7(3)
O(41)–Ni(2)–O(61)	67.73(10)	O(41)–Zn(2)–O(61)	64.5(2)	N(1)–Ni(1)–N(23)	89.9(3)
O(41)–Ni(2)–N(1)	161.04(12)	O(41)–Zn(2)–N(1)	157.7(2)	N(19)–Ni(1)–N(23)	100.3(3)
O(41)–Ni(2)–N(2)	90.62(13)	O(41)–Zn(2)–N(2)	89.6(2)	O(11)–Zn(2)–O(31)	83.7(2)
O(61)–Ni(2)–N(1)	95.49(12)	O(61)–Zn(2)–N(1)	96.2(2)	O(11)–Zn(2)–O(41)	129.1(2)
O(61)–Ni(2)–N(2)	95.95(12)	O(61)–Zn(2)–N(2)	97.9(2)	O(11)–Zn(2)–O(61)	119.5(2)
N(1)–Ni(2)–N(2)	100.22(15)	N(1)–Zn(2)–N(2)	104.7(2)	O(31)–Zn(2)–O(41)	119.8(2)
O(41)–Ni(3)–O(61)	78.06(11)	O(41)–Ni(3)–O(61)	78.3(2)	O(31)–Zn(2)–O(61)	126.1(2)
O(41)–Ni(3)–N(49)	93.25(14)	O(41)–Ni(3)–N(49)	93.1(2)	O(41)–Zn(2)–O(61)	84.3(2)
O(41)–Ni(3)–N(53)	170.46(13)	O(41)–Ni(3)–N(53)	170.3(2)	O(4)–Ni(3)–O(41)	86.4(2)
O(61)–Ni(3)–N(49)	170.79(14)	O(61)–Ni(3)–N(49)	170.7(2)	O(4)–Ni(3)–O(61)	87.1(2)
O(61)–Ni(3)–N(53)	92.42(13)	O(61)–Ni(3)–N(53)	92.1(2)	O(4)–Ni(3)–N(2)	178.4(3)
N(49)–Ni(3)–N(53)	96.29(15)	N(49)–Ni(3)–N(53)	96.6(2)	O(4)–Ni(3)–N(49)	90.7(2)
				O(4)–Ni(3)–N(53)	84.6(2)
				O(41)–Ni(3)–O(61)	79.6(2)
				O(41)–Ni(3)–N(2)	95.2(3)
				O(41)–Ni(3)–N(49)	89.6(2)
				O(41)–Ni(3)–N(53)	166.8(2)
				O(61)–Ni(3)–N(2)	92.8(2)
				O(61)–Ni(3)–N(49)	169.0(2)
				O(61)–Ni(3)–N(53)	90.3(2)
				N(2)–Ni(3)–N(49)	89.8(3)
				N(2)–Ni(3)–N(53)	93.8(3)
				N(49)–Ni(3)–N(53)	100.2(3)

metal coordination spheres are given in Table 3. The molecular structure of **3** consists of the neutral trinuclear unit  $[(\text{NiL})_2\text{Zn}(\text{NCS})_2(\text{CH}_3\text{OH})_2]$  and two noncoordinated methanol molecules. In this trinuclear unit, the three metal atoms (two terminal Ni atoms and the central Zn atom) are in a nearly linear disposition. Thus, the geometry is very different from that observed in **1** and **2**. The two terminal Ni(II) ions present

a distorted octahedral coordination sphere. The basal plane of each Ni(II) ion is formed by the two imine nitrogen atoms and two phenoxido oxygen atoms from one “metallo ligand”. These four donors in the equatorial plane show root-mean-squared deviations from their mean planes of 0.044 and 0.056 Å for Ni1 and Ni3, respectively. The metal atoms are displaced 0.082(3) and 0.099(3) Å from the mean plane in the direction of axial



**Figure 3.** Structure of complex 3 with ellipsoids at 30% probability. Two noncoordinated methanol molecules are not shown.

atoms N1 and O4 for Ni1 and Ni3, respectively. The basal Ni–O and Ni–N bond distances are in similar ranges (Table 3). The apical positions are occupied by the nitrogen atoms from a  $\kappa\text{N-SCN}^-$  anion and by an oxygen atom from a coordinated methanol molecule. The apical Ni–O and Ni–N bond lengths are also in similar ranges and the axial trans angles are close to  $180^\circ$  (Table 3). In contrast to **1** and **2**, the orientation of the two  $\text{SCN}^-$  ligands is similar with Ni–N–C bond angles of  $167.9(87)$  and  $170.1(7)^\circ$ . Again, in contrast to **1** and **2**, the dihedral angle between the two  $\text{N}_2\text{–Ni–O}_2$  planes is  $77.7(1)^\circ$ , indicating that the two “metalloligands” are almost perpendicular (Figure 3).

Another remarkable difference between **1** and **2** from **3** is the tetrahedral environment of the Zn(II) ion, which is bonded to four bridging phenoxido oxygen atoms from two different [NiL] units. The four Zn–O bonds lengths are very similar (in the range  $1.947(5)$ – $1.956(5)$  Å, Table 3) forming a distorted-tetrahedral with O–Zn–O bond angles in the range  $83.7(2)$ – $129.1(2)^\circ$  (Table 3). The distorted tetrahedral geometry around the Zn(II) ion is confirmed by its  $\tau_4$  index of 0.74 and by the dihedral angle of  $82.6(2)^\circ$  between the two O–Zn–O planes. The dihedral angle is  $0^\circ$  for a perfectly square planar arrangement and  $90^\circ$  for a perfect tetrahedral arrangement. The

Ni1...Zn2 and Ni3...Zn2 distances are  $3.032(1)$  and  $3.024(1)$  Å and the Ni1...Ni3 distance is  $6.056(2)$  Å. In contrast to **1** and **2**, the three metal atoms in the trinuclear unit are nearly linear as is evident from the Ni1–Zn2–Ni3 angle ( $178.93(4)^\circ$ ).

As in **1** and **2**, some noncovalent H-bonding and C–H... $\pi$  interactions are present in complex **3** (see Figure S11, Supporting Information).

Complexes **2** and **3** represent rare examples of very closely related  $\text{Ni}_2\text{Zn}$  complexes having different spatial arrangements (bent, nearly orthogonal in **2** and almost linear in **3**, Figure 4). These different arrangements arise from the different coordination environments of the Ni(II) and Zn(II) ions: the terminal Ni(II) ions are square planar in **2** but octahedral in **3**. The central Zn(II) ion also presents different coordination spheres: octahedral in **2** and tetrahedral in **3** (Figure 4). It should be noted that the occurrence of linear and bent molecular geometries in trinuclear compounds is very rare and only recently has it been found in a couple of isomers with a similar Schiff base.<sup>41</sup> The comparable energy of stabilization in both geometries of Zn(II) (tetrahedral and octahedral) due to the lack of crystal field stabilization may explain the presence of these two closely related  $\text{Ni}_2\text{Zn}$  complexes with so different coordination environments.

A search in the CCDC database (updated May 2013) shows a total of ca. 30 trinuclear compounds formed by transition metals and group 12 metals with Schiff bases and  $\kappa\text{-N}$  or  $\kappa\text{-S}$   $\text{SCN}^-$  ligands.<sup>34–37,47,64–74</sup> Only four present a linear geometry (as observed in **3**): two  $\text{Cu}_2\text{Hg}$  trinuclear complexes (with the  $\text{SCN}^-$  ligand, as expected,  $\kappa\text{-S}$  coordinated to the central soft Hg atom),<sup>75</sup> one  $\text{Cd}_3$  trinuclear complex<sup>72</sup> and one  $\text{Zn}_3$  trinuclear complex.<sup>76</sup> In the latter two compounds, each of the terminal metal atoms bears a coordinated  $\text{SCN}^-$  ligand ( $\kappa\text{-S}$  for Cd and  $\kappa\text{-N}$  for Zn, in agreement with the softer character of Cd). Complex **3** is, therefore, the first linear compound of this type that contains Ni(II) ions.

The structure of the two independent complexes of **4** is shown in Figure 5 together with the atomic numbering scheme. Selected bond lengths and angles are summarized in Table 4. The molecular structure of the cocrystal **4** contains two discrete neutral trinuclear units  $[(\text{NiL})_2\text{Zn}(\text{NCS})_2(\text{CH}_3\text{OH})_2]$  (named **4A**) and  $[(\text{NiL})_2\text{Zn}(\text{NCS})_2]$  (named **4B**) together with two

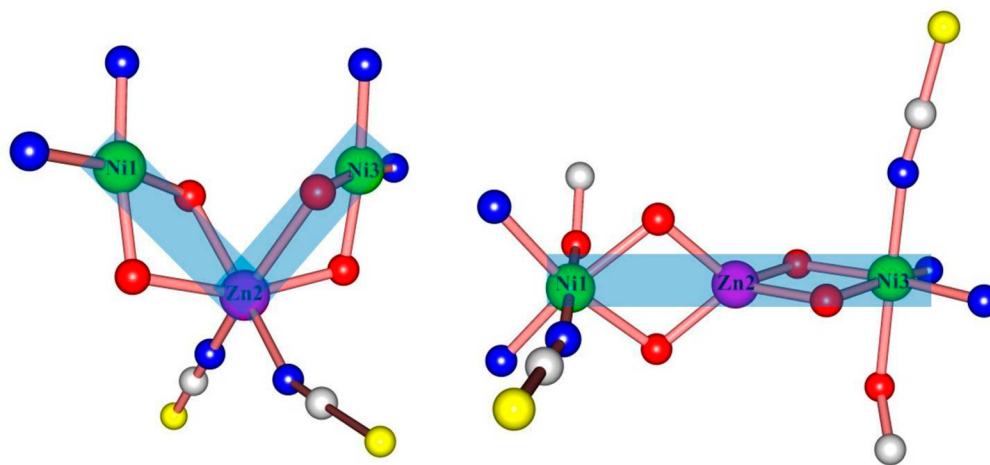


**Figure 4.** Coordination environments of complexes of **2** (left) and **3** (right). The bent arrangement of three metal atoms of complex **2** and the linearity of three metal atoms of complex **3** are indicated by the light blue shadows. Note that **1** is isostructural with **2**. Color code: O = red, N = blue, C = white, S = yellow.

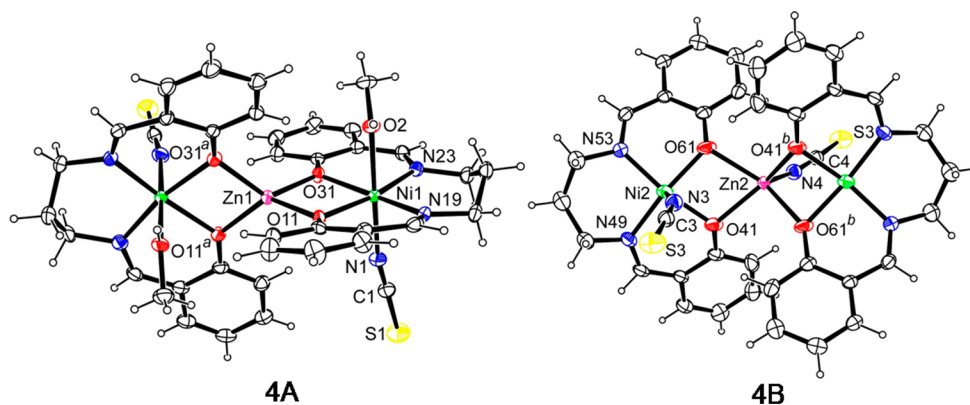


**Figure 5.** Structure of the two independent complexes (both located on a 2-fold axis) of complex 4 with ellipsoids at 30% probability (symmetry transformation  $^a = 1 - x, y, 1/2 - z$  for 4A and  $^b = 3/2 - x, 1/2 - y, 2 - z$  for 4B). Two noncoordinated water molecules are not shown here.

**Table 4. Bond Distances (Å) and Angles (deg) for Complex 4**

complex 4A		complex 4B	
Ni(1)–O(2)	2.159(4)	Ni(2)–N(3)	2.048(9)
Ni(1)–O(11)	2.038(3)	Ni(2)–O(41)	1.928(5)
Ni(1)–O(31)	2.044(3)	Ni(2)–O(61)	1.929(5)
Ni(1)–N(1)	2.057(5)	Ni(2)–N(49)	1.941(5)
Ni(1)–N(19)	2.019(4)	Ni(2)–N(53)	1.933(4)
Ni(1)–N(23)	2.022(4)	Zn(2)–N(4)	1.943(9)
Zn(1)–O(11)	1.946(3)	Zn(2)–O(41)	2.126(4)
Zn(1)–O(31)	1.953(3)	Zn(2)–O(61)	2.140(4)
O(2)–Ni(1)–N(19)	90.54(15)	N(3)–Ni(2)–N(49)	97.4(3)
O(2)–Ni(1)–O(11)	87.74(14)	N(3)–Ni(2)–N(53)	103.6(3)
O(2)–Ni(1)–O(31)	84.22(13)	N(3)–Ni(2)–O(41)	89.5(3)
O(2)–Ni(1)–N(1)	177.50(16)	N(3)–Ni(2)–O(61)	90.2(3)
O(2)–Ni(1)–N(23)	87.58(16)	O(41)–Ni(2)–O(61)	80.74(18)
O(11)–Ni(1)–O(31)	79.30(12)	O(41)–Ni(2)–N(49)	90.99(18)
O(11)–Ni(1)–N(1)	92.50(15)	O(41)–Ni(2)–N(53)	164.23(18)
O(11)–Ni(1)–N(19)	90.80(14)	O(61)–Ni(2)–N(53)	90.39(18)
O(11)–Ni(1)–N(23)	168.68(14)	O(61)–Ni(2)–N(49)	168.75(19)
O(31)–Ni(1)–N(1)	93.37(14)	N(49)–Ni(2)–N(53)	95.86(18)
O(31)–Ni(1)–N(19)	168.94(14)	O(41)–Zn(2)–O(61)	71.69(15)
O(31)–Ni(1)–N(23)	89.98(15)	O(41)–Zn(2)–O(41) <sup>b*</sup>	135.12(19)
N(1)–Ni(1)–N(19)	91.95(16)	O(41)–Zn(2)–O(61) <sup>b</sup>	90.80(16)
N(1)–Ni(1)–N(23)	91.74(17)	O(41)–Zn(2)–N(4)	104.5(3)
N(19)–Ni(1)–N(23)	99.55(16)	O(61)–Zn(2)–O(41) <sup>b</sup>	92.68(16)
O(11)–Zn(1)–O(31)	83.82(12)	O(61)–Zn(2)–O(61) <sup>b</sup>	136.19(18)
O(11)–Zn(1)–O(11) <sup>a*</sup>	127.58(12)	O(61)–Zn(2)–N(4)	104.3(3)
O(11)–Zn(1)–O(31) <sup>a</sup>	118.62(12)	O(41) <sup>b</sup> –Zn(2)–N(4)	120.2(3)
O(31)–Zn(1)–O(31) <sup>a</sup>	130.30(12)	O(61) <sup>b</sup> –Zn(2)–N(4)	119.1(3)
		O(61) <sup>b</sup> –Zn(2)–O(41) <sup>b</sup>	71.59(16)

\*Symmetry elements:  $^a = 1 - x, y, 1/2 - z$  for 4A;  $^b = 3/2 - x, 1/2 - y, 2 - z$  for 4B.

disordered water molecules. Both trinuclear units have a crystallographic 2-fold axis. The structure of the trinuclear unit 4A is identical to that in 3 with all the donor atoms in the coordination spheres of the terminal Ni and central Zn centers similarly bonded. All the Ni–O and Ni–N bond lengths are very similar (Table 4). Again, the root-mean-squared deviation of these four donor atoms in the basal plane around the Ni center is 0.010 Å while the metal atom deviates 0.083(1) Å from this plane in the direction of the N1 atom. The dihedral angle between the two N<sub>2</sub>–Ni–O<sub>2</sub> planes is 79.53°. The central Zn atom possesses a distorted-tetrahedral geometry ( $\tau_4 = 0.71$ ) with a dihedral angle between the two O–Zn–O planes of 80.39°, very similar, as expected, to the angle between the N<sub>2</sub>–

Ni–O<sub>2</sub> planes. Like in 3, the Zn–O bond lengths are very close and the O–Zn–O bond angles are in the range 83.82(12)–130.30(12)°. The Ni1...Zn1 and Ni1...Ni1<sup>a</sup> distances are 3.022(2) and 6.044(4) Å, respectively, and the Ni1–Zn1–Ni1<sup>a</sup> angle is 178.77(3)°, indicating an almost perfect linear arrangement of the three metal ions.

The other trinuclear unit (4B), although it has a similar molecular shape to 4A (almost linear Ni<sub>2</sub>Zn unit), presents different coordination environments for the metal atoms (Figure 5). Interestingly, 4B and complex 2 are “coordination position isomers” because they have the same formula: [(NiL)<sub>2</sub>Zn(SCN)<sub>2</sub>] but present a different distribution of the thiocyanato ligands. Thus, in 4B, one of the two terminal Ni



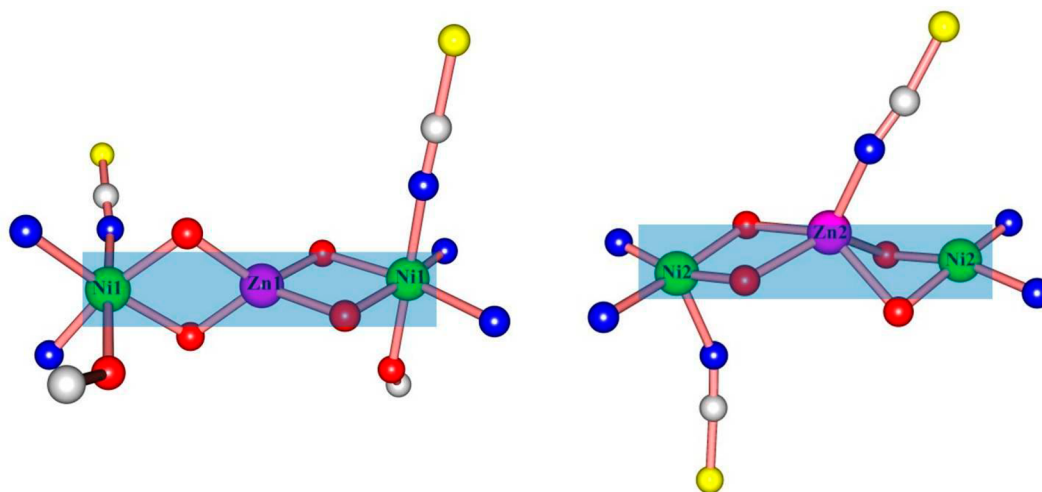


**Figure 6.** The two  $\text{Ni}_2\text{Zn}$  trinuclear units in the cocrystal **4**. The linearity of three metal atoms is shown by light blue shadow (left, **4A**; right, **4B**). Color code: O = red, N = blue, C = white, S = yellow.

atoms is square planar whereas the other is square pyramidal although there is a positional disorder with occupancy of 1/2 in such a way that in half of the complexes the  $\kappa\text{N-SCN}^-$  ligand is coordinated to one Ni(II) ion and in the other half it is coordinated to the other (because the two terminal Ni atoms are equivalent due to the  $\text{C}_2$  axis). The central atom is a Zn(II) atom with a square pyramidal geometry. In **2**, the two terminal Ni(II) ions are square planar and the central Zn(II) is octahedral. The basal plane of the two terminal Ni(II) ions in **4B** is formed by the two imine N atoms and the two phenoxido O atoms of the Schiff base. The Ni–O and Ni–N bond lengths in the basal plane are slightly shorter than in **3** and **4A** (Tables 3 and 4). A  $\kappa\text{N-SCN}^-$  anion completes the square pyramidal geometry of the terminal Ni(II) atoms occupying the axial position in both Ni2 atoms with an occupancy factor of 1/2. The square pyramidal geometry around Ni(2) is slightly distorted, as indicated by the Addison parameter ( $\tau = 0.075$ ). The  $\tau$  is 0 for an ideal square pyramid and 1 for a trigonal bipyramid.<sup>77</sup> The central Zn(II) ions presents a square pyramidal coordination sphere where the basal plane is constituted by the four bridging phenoxido oxygen atoms of the two different [NiL] “metalloligands”. An axial  $\kappa\text{N-SCN}^-$  ion completes the square pyramidal geometry. The low Addison parameter of the Zn(II) atom ( $\tau = 0.018$ ) indicates a very small distortion of the square pyramidal geometry.

A surprising fact in the structure of **4** is the presence of two different (although related) complexes (**4A** and **4B**, Figure 6), one of them (**4A**) being identical to complex **3** and the other one (**4B**) being a “coordination position isomer” of complex **2**. As far as we know, this is the first example of a cocrystal formed by a trinuclear unit (**4A**) that may crystallize as an isolated trinuclear unit (**3**) and a second trinuclear unit (**4B**), which is a “coordination position isomer” of another trinuclear unit (**2**) that can also be isolated.

Another surprising finding is the existence of up to three different, although closely related,  $\text{Ni}_2\text{Zn}$  trinuclear units formed with the same [NiL] complex, Zn(II) and  $\text{SCN}^-$ . This fact suggests that the different linear and bent trinuclear units have very small differences in energy. Although the driving force to obtain complexes **2**, **3**, **4A** and **4B** seems to be the [NiL]:Zn(II): $\text{SCN}^-$  ratio (Scheme 1), there must be other factors determining the crystallized trinuclear unit because

complex **3** is isolated for a [NiL] concentration four times higher than for complex **4A** (whose structure is identical to **3**). Surprisingly, the use of intermediate concentrations does not yield the linear complexes **3**, **4A** nor **4B** instead, the bent one (**2**). Interestingly, if we replace Zn(II) by Ni(II), we always observe the bent complex **1** (isostructural to **2**). This observation indicates that the central Ni(II) ion prefers the octahedral geometry (as in **1**) in contrast with Zn(II) that may present different geometries: octahedral (in **2**), tetrahedral (in **3** and **4A**) and square pyramidal (in **4B**), in agreement with the lack of energy of stabilization of the crystal field in Zn(II) complexes for any geometry with only  $\sigma$  bonds ( $d^{10}$  ion).

**Magnetic Measurements of the Complexes.** Because the X-ray structure determination does not allow an unambiguous assignment of the Zn(II) and Ni(II) centers (as they have similar electron densities), we have performed magnetic measurements in complexes **1–4** to determine the exact nature of each metal center in each trinuclear unit.

The thermal variation of the  $\chi_m T$  product for complex **1** per  $\text{Ni}_3$  unit shows at room temperature a value of ca.  $1.2 \text{ emu}\cdot\text{K}\cdot\text{mol}^{-1}$ , which is the expected value for a  $S = 1$  Ni(II) ion with a  $g$  value of ca. 2.2. When the temperature is lowered,  $\chi_m T$  remains constant down to ca. 10 K (Figure 7). Below ca. 10 K,  $\chi_m T$  shows an abrupt decrease to reach a value of ca.  $0.4 \text{ emu}\cdot\text{K}\cdot\text{mol}^{-1}$  at 2 K. This behavior indicates that complex **1** presents

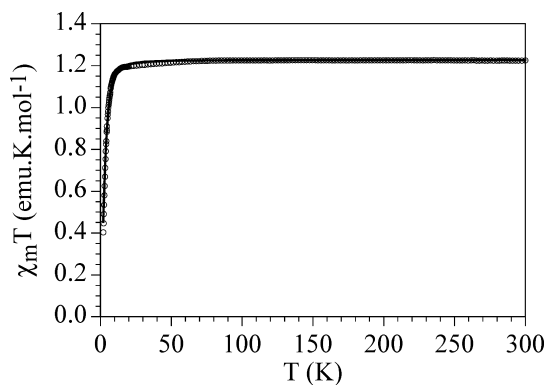


**Figure 7.** Thermal variation of the  $\chi_m T$  product per  $\text{Ni}_3$  trinuclear unit for complex **1**. Solid line is the best fit to the model (see text).

only one paramagnetic Ni(II) center (the octahedral central one) and, therefore, the two terminal Ni(II) ions are diamagnetic, in agreement with their square planar geometry ( $d^8$  configuration). Accordingly, the magnetic properties of **1** have been fitted to a simple isolated  $S = 1$  monomer with a zero field splitting (ZFS). The fit is very satisfactory in the whole temperature range (solid line in Figure 7) with  $g = 2.216$  and  $|D| = 7.4 \text{ cm}^{-1}$ .

Complex **2** is diamagnetic, as expected from its structure that shows a central octahedral diamagnetic Zn(II) ion and two terminal square planar diamagnetic Ni(II) ions.

The thermal variation of  $\chi_m T$  for complex **3** per  $\text{Ni}_2\text{Zn}$  unit shows a room temperature value of ca.  $2.4 \text{ emu}\cdot\text{K}\cdot\text{mol}^{-1}$ , close to the expected value for two isolated  $S = 1$  Ni(II) ions with a  $g$  value of ca. 2.2. When the temperature is lowered,  $\chi_m T$  remains constant down to ca. 10 K (Figure 8). Below ca. 10 K,  $\chi_m T$

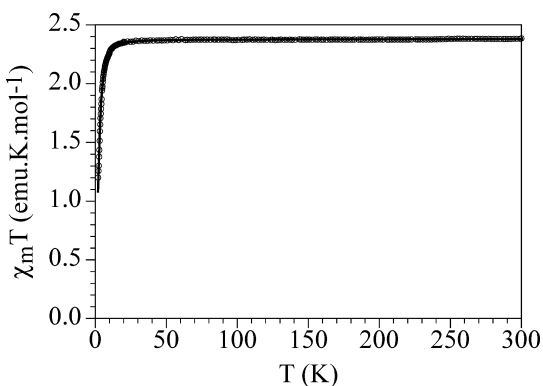


**Figure 8.** Thermal variation of the  $\chi_m T$  product per  $\text{Ni}_2\text{Zn}$  trinuclear unit for complex **3**. Solid line is the best fit to the model (see text).

shows an abrupt decrease and reaches a value of ca.  $1.2 \text{ emu}\cdot\text{K}\cdot\text{mol}^{-1}$  at 2 K. This behavior indicates that complex **3** presents two isolated paramagnetic Ni(II) centers (the octahedral terminal ones) in agreement with its structure. Accordingly, the magnetic properties of **3** have been fitted to a model for two isolated  $S = 1$  monomers with a ZFS. This model reproduces very satisfactorily the magnetic properties of **3** in the whole temperature range with  $g = 2.179$  and  $|D| = 6 \text{ cm}^{-1}$  (solid line in Figure 8).

The thermal variation of  $\chi_m T$  per formula unit for **4** (containing two trinuclear  $\text{Ni}_2\text{Zn}$  units, **4A** and **4B**) shows a room temperature  $\chi_m T$  value of ca.  $3.5 \text{ emu}\cdot\text{K}\cdot\text{mol}^{-1}$ , which is the expected value for three isolated  $S = 1$  Ni(II) ions with  $g \approx 2.2$ . This  $\chi_m T$  value remains constant down to ca. 30 K, and below this temperature, it shows a sharp decrease and reaches a value of ca.  $1.1 \text{ emu}\cdot\text{K}\cdot\text{mol}^{-1}$  at 2 K (Figure 9). This behavior indicates that **4** presents a total of 3 paramagnetic Ni(II) ions per formula unit. Since **4A** is identical to complex **3**, we can assume that the contribution of this trinuclear unit **4A** must be ca.  $2.4 \text{ emu}\cdot\text{K}\cdot\text{mol}^{-1}$  (as in **3**) and that the remaining ca.  $1.1 \text{ emu}\cdot\text{K}\cdot\text{mol}^{-1}$  must be the contribution of **4B**. This value agrees with the observed structure of **4B** that, besides the diamagnetic central Zn(II) ions, shows a diamagnetic square planar Ni(II) ion and a paramagnetic square pyramidal Ni(II) ion. Accordingly, we have fitted the magnetic properties to a model consisting in three isolated  $S = 1$  monomers with the same ZFS parameter (to reduce the number of adjustable parameters). This model reproduces very satisfactorily the magnetic properties of **4** with  $g = 2.056$  and  $|D| = 12.2 \text{ cm}^{-1}$ .

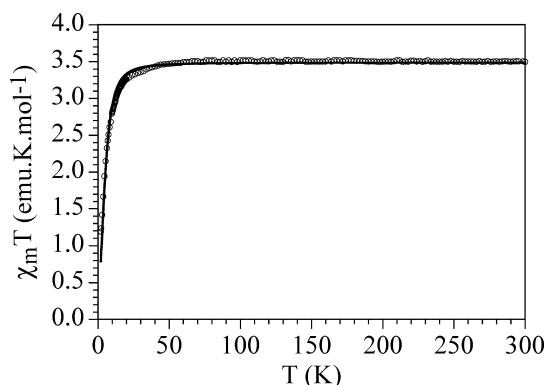


**Figure 9.** Thermal variation of the  $\chi_m T$  product per formula unit (two  $\text{Ni}_2\text{Zn}$  trinuclear units) for complex **4**. Solid line is the best fit to the model (see text).

Note that the fit at low temperatures slightly deviates from the experimental points, probably due to the assumption that the three Ni(II) ions present the same ZFS. Because the magnetic measurements have been performed on powdered samples, we cannot determine the sign of the ZFS parameter in neither of the three compounds.

## CONCLUSIONS

In the present work, we have shown that the complex formed with Ni(II) and the tetradentate Schiff base ligand  $N,N'$ -bis(salicylidene)-1,3-propanediamine, [NiL], may act as a “metalloligand” toward Ni(II) and Zn(II) ions to produce different types of  $\text{Ni}_3$  (**1**) and  $\text{Ni}_2\text{Zn}$  trinuclear compounds (**2**, **3** and **4**) with  $\text{SCN}^-$  as a coligand. One of the most surprising results is that by simply changing the [NiL] concentration, up to three different  $\text{Ni}_2\text{Zn}$  compounds with very close compositions but different geometries can be isolated, namely the bent species  $[(\text{NiL})_2\text{Zn}(\text{NCS})_2]$  (**2**), the linear ones  $[(\text{NiL})_2\text{Zn}(\text{NCS})_2(\text{CH}_3\text{OH})_2]$  (**3** and **4A**) and  $[(\text{NiL})_2\text{Zn}(\text{NCS})_2]$  (**4B**). Interestingly, the bent complex is the only one obtained as a  $\text{Ni}_3$  trinuclear unit (**1**).

But the most interesting and unexpected result is the formation of complex **4**, which is a cocrystal formed by two different  $\text{Ni}_2\text{Zn}$  trinuclear units (**4A** and **4B**). **4A** is identical to complex **3** whereas **4B** is a “coordination position isomer” of complex **2**. This unusual result, a cocrystal formed by an existing complex and a “coordination position isomer” of another existing complex is, as far as we know, unprecedented in coordination chemistry. The “coordination position isomer” between **2** and **4B** is raised due to the migration of one  $\text{SCN}^-$  ligand from the central octahedral Zn(II) ion to one of the square planar terminal Ni(II) ions. The flexibility of the coordination numbers of Ni(II) and Zn(II) ions seems to play the crucial role in obtaining these isomers. Moreover, the observation of the “coordination position isomers” with  $\text{SCN}^-$  anions proves that it can produce isomers other than the well-known “linkage” isomers.

## ASSOCIATED CONTENT

### Supporting Information

Figures of powder XRD pattern, IR spectra and ESI mass spectra of the complexes (Figures S1–S11), the non-covalent interactions present in the complexes **1–3**, electrospray ionization mass spectrometry of complexes **2–4** and crystallographic data in CIF format for all four complexes (**1–4**). This

material is available free of charge via the Internet at <http://pubs.acs.org>.

## AUTHOR INFORMATION

### Corresponding Author

\*A. Ghosh. E-mail: [ghosh\\_59@yahoo.com](mailto:ghosh_59@yahoo.com).

### Notes

The authors declare no competing financial interest.

## ACKNOWLEDGMENTS

L. K. Das and A. Biswas are thankful to CSIR, India for awarding Senior Research Fellowship [Sanction No. 09/028 (0805)/2010-EMR-I for L. K. Das and 09/028 (0717)/2008-EMR-I for A. Biswas]. We also acknowledge the Spanish MINECO (project MAT2011-26507) and the Generalitat Valenciana (Prometeo and ISIC Programs) for financial support. Thanks are given to the Consejo Superior de Investigaciones Científicas (CSIC) of Spain for the award of a license for the use of the Cambridge Crystallographic Data Base (CSD). Crystallography was performed at the DST-FIST, India funded Single Crystal Diffractometer Facility at the Department of Chemistry, University of Calcutta. The authors also thank the Department of Science and Technology (DST), New Delhi, India, for financial support (SR/S1/IC/0034/2012).

## REFERENCES

- (1) (a) Bernstein, J. *Cryst. Growth Des.* **2011**, *11*, 632–650. (b) Aakeroy, C. B.; Champness, N. R.; Janiak, C. *CrystEngComm* **2010**, *12*, 22–43.
- (2) Bishop, R. *Acc. Chem. Res.* **2009**, *42*, 67–78.
- (3) Nangia, A. *J. Chem. Sci.* **2010**, *122*, 295–310.
- (4) Habgood, M.; Price, S. L. *Cryst. Growth Des.* **2010**, *10*, 3263–3272.
- (5) Moulton, B.; Zaworotko, M. J. *Chem. Rev.* **2001**, *101*, 1629–1658.
- (6) (a) Stahly, G. P. *Cryst. Growth Des.* **2007**, *7*, 1007–1026. (b) Desiraju, G. R. *Angew. Chem., Int. Ed.* **2007**, *46*, 8342–8356. (c) Benmansour, S.; Marchivie, M.; Triki, S.; Gómez-García, C. J. *Crystals* **2012**, *2*, 306–326.
- (7) Kettle, S. F. A. *Physical Inorganic Chemistry*; Oxford University Press: Oxford, U.K., 2000; pp 43–44.
- (8) Benmansour, S.; Setifi, F.; Triki, S.; Gómez-García, C. J. *Inorg. Chem.* **2012**, *51*, 2359–2365.
- (9) Kauffman, G. B. *J. Chem. Educ.* **1959**, *36*, 521–527.
- (10) Werner, A.; King, V. L. *Ber. Dtsch. Chem. Ges.* **1911**, *44*, 1887–1898.
- (11) Yonemura, M.; Arimura, K.; Inoue, K.; Usuki, N.; Ohba, M.; Ohkawa, H. *Inorg. Chem.* **2002**, *41*, 582–589.
- (12) Childs, S. L.; Zaworotko, M. J. *Cryst. Growth Des.* **2009**, *9*, 4208–4211.
- (13) Arenas-García, J. I.; Herrera-Ruiz, D.; Mondragón-Vásquez, K.; Morales-Rojas, H.; Höpfl, H. *Cryst. Growth Des.* **2012**, *12*, 811–824.
- (14) Puigjaner, C.; Barbas, R.; Portell, A.; Valverde, I.; Vila, X.; Alcob, X.; Font-Bardia, M.; Prohens, R. *CrystEngComm* **2012**, *14*, 362–365.
- (15) Aitipamula, S.; Banerjee, R.; Bansal, A. K.; Biradha, K.; Cheney, M. L.; Choudhury, A. R.; Desiraju, G. R.; Dikundwar, A. G.; Dubey, R.; Duggirala, N.; Ghogale, P. P.; Ghosh, S.; Goswami, P. K.; Goud, N. R.; Jetti, R. R. K. R.; Karpinski, P.; Kaushik, P.; Kumar, D.; Kumar, V.; Moulton, B.; Mukherjee, A.; Mukherjee, G.; Myerson, A. S.; Puri, V.; Ramanan, A.; Rajamannar, T.; Reddy, C. M.; Rodriguez-Hornedo, N.; Rogers, R. D.; Row, T. N. G.; Sanphui, P.; Shan, N.; Shete, G.; Singh, A.; Sun, C. C.; Swift, J. A.; Thaimattam, R.; Thakur, T. S.; Thaper, R. K.; Thomas, S. P.; Tothadi, S.; Vangala, V. R.; Variankaval, N.; Vishweshwar, P.; Weyna, D. R.; Zaworotko, M. J. *Cryst. Growth Des.* **2012**, *12*, 2147–2152.
- (16) Datta, J.; Nandi, A. K. *Polymer* **1994**, *35*, 4804–4812.
- (17) Koshima, H.; Nagano, M.; Asahi, T. *J. Am. Chem. Soc.* **2005**, *127*, 2455–2463.
- (18) Childs, S. L.; Chyall, L. J.; Dunlap, J. T.; Smolenskaya, V. N.; Stahly, B. C.; Stahly, G. P. *J. Am. Chem. Soc.* **2004**, *126*, 13335–13342.
- (19) Remenar, J. F.; Morissette, S. L.; Peterson, M. L.; Moulton, B.; MacPhee, J. M.; Guzman, H. R.; Almarsson, O. *J. Am. Chem. Soc.* **2003**, *125*, 8456–8457.
- (20) Zhang, X.-L.; Chen, X.-M. *Cryst. Growth Des.* **2005**, *5*, 617–622.
- (21) Akpinar, H.; Mague, J. T.; Novak, M. A.; Friedmann, J. R.; Lahti, P. M. *CrystEngComm* **2012**, *14*, 1515–1526.
- (22) Keyes, T. E.; Forster, R. J.; Bond, A. M.; Miao, W. *J. Am. Chem. Soc.* **2001**, *123*, 2877–2884.
- (23) Koshima, H.; Miyamoto, H.; Yagi, I.; Uosaki, K. *Cryst. Growth Des.* **2004**, *4*, 807–811.
- (24) Ohba, S.; Hosomi, H.; Ito, Y. *J. Am. Chem. Soc.* **2001**, *123*, 6349–6356.
- (25) Loehlin, J. H.; Etter, M. C.; Gendreau, C.; Cervasio, E. E. *Chem. Mater.* **1994**, *6*, 1218–1221.
- (26) Wang, X.-L.; Guo, Z.-C.; Liu, G.-C.; Qu, Y.; Yang, S.; Lin, H.-Y.; Zhang, J.-W. *CrystEngComm* **2013**, *15*, 551–559.
- (27) Bhogala, B. R.; Nangia, A. *Cryst. Growth Des.* **2003**, *3*, 547–554.
- (28) Mukherjee, P.; Drew, M. G. B.; Gómez-García, C. J.; Ghosh, A. *Inorg. Chem.* **2009**, *48*, 4817–4827.
- (29) Lee, H. M.; Olmstead, M. M.; Gross, G. G.; Balch, A. L. *Cryst. Growth Des.* **2003**, *3*, 691–697.
- (30) Olmstead, M. M.; Wei, P.; Ginwalla, A. S.; Balch, A. L. *Inorg. Chem.* **2000**, *39*, 4555–4559.
- (31) Chou, C.-C.; Su, C.-C.; Tsai, H.-L.; Lii, K.-H. *Inorg. Chem.* **2005**, *44*, 628–632.
- (32) Palaniandavar, M.; Butcher, R. J.; Addison, A. W. *Inorg. Chem.* **1996**, *35*, 467–471.
- (33) Fernandes, J. A.; Ramos, A. I.; Braga, S. S.; Paz, F. A. A. *Acta Crystallogr., Sect. E: Struct. Rep. Online* **2010**, *E66*, m1689–m1690.
- (34) Biswas, S.; Ghosh, A. *Polyhedron* **2011**, *30*, 676–681.
- (35) Das, L. K.; Drew, M. G. B.; Ghosh, A. *Inorg. Chim. Acta* **2013**, *394*, 247–254.
- (36) Das, L. K.; Biswas, A.; Frontera, A.; Ghosh, A. *Polyhedron* **2013**, *52*, 1416–1424.
- (37) Biswas, S.; Naiya, S.; Gómez-García, C. J.; Ghosh, A. *Dalton trans.* **2012**, *41*, 462–473.
- (38) Biswas, S.; Ghosh, A. *Indian J. Chem., Sect. A: Inorg., Bio-inorg., Phys., Theor. Anal. Chem.* **2011**, *50A*, 1356–1362.
- (39) Das, L. K.; Kadam, R. M.; Bauzá, A.; Frontera, A.; Ghosh, A. *Inorg. Chem.* **2012**, *51*, 12407–12418.
- (40) Das, L. K.; Ghosh, A. *CrystEngComm* **2013**, *15*, 9444–9456.
- (41) Das, L. K.; Park, S.-W.; Cho, S. J.; Ghosh, A. *Dalton Trans.* **2012**, *41*, 11009–11017.
- (42) You, Z.-L.; Zhu, H.-L. *Z. Anorg. Allg. Chem.* **2004**, *630*, 2754–2760.
- (43) Novitchi, G.; Shova, S.; Caneschi, A.; Costes, J.-P.; Gdaniec, M.; Stanica, N. *Dalton Trans.* **2004**, 1194–1200.
- (44) (a) Shakya, R.; Jozwiuk, A.; Powell, D. R.; Houser, R. P. *Inorg. Chem.* **2009**, *48*, 4083–4088. (b) Yildirim, L. T.; Ergun, U. *Acta Crystallogr.* **2007**, *E63*, m2424–m2425. (c) Ercan, F.; Ates, M. B.; Ercan, Y.; Durmus, S.; Atakol, O. *Cryst. Res. Technol.* **2004**, *39*, 470–476.
- (45) Biswas, S.; Saha, R.; Ghosh, A. *Organometallics* **2012**, *31*, 3844–3850.
- (46) Epstein, J. M.; Figgis, B. N.; White, A. H.; Willis, A. C. *J. Chem. Soc., Dalton Trans.* **1974**, 1954–1961.
- (47) Ercan, F.; Atakol, O. *Z. Kristallogr.* **2006**, *221*, 735–739.
- (48) Song, Y.-F.; Albada, G. A. V.; Tang, J.; Mutikainen, I.; Turpeinen, U.; Massera, C.; Roubeau, O.; Costa, J. S.; Gamez, P.; Reedijk, J. *Inorg. Chem.* **2007**, *46*, 4944–4950.
- (49) Ates, B. M.; Ercan, F.; Svoboda, I.; Fuess, H.; Atakol, O. *Acta Crystallogr., Sect. E: Struct. Rep. Online* **2008**, *64*, m481–m482.
- (50) Biswas, S.; Ghosh, A. *Polyhedron* **2011**, *65*, 322–331.
- (51) Atakol, O.; Nazir, H.; Arici, C.; Durmus, S.; Svoboda, I.; Fuess, H. *Inorg. Chim. Acta* **2003**, *342*, 295–300.

- (52) Bain, G. A.; Berry, J. F. *J. Chem. Educ.* **2008**, *85*, 532–536.
- (53) SAINTE, version 6.02; SADABS, version 2.03; BrukerAXS, Inc., Madison, WI, 2002.
- (54) Sheldrick, G. M. *SHELXS 97, Program for Structure Solution*; University of Göttingen, Germany, 1997.
- (55) Sheldrick, G. M. *SHELXL 97, Program for Crystal Structure Refinement*; University of Göttingen, Germany, 1997.
- (56) Spek, A. L. *J. Appl. Crystallogr.* **2003**, *36*, 7–13.
- (57) Farrugia, L. J. *J. Appl. Crystallogr.* **1999**, *32*, 837–838.
- (58) Farrugia, L. J. *J. Appl. Crystallogr.* **1997**, *30*, 565.
- (59) Ferguson, J. *J. Chem. Phys.* **1961**, *34*, 611–615.
- (60) Sigalas, M. P.; Tsipis, C. A. *Inorg. Chem.* **1986**, *25*, 1875–1880.
- (61) Dey, M.; Rao, C. P.; Saarenketo, P. K.; Rissanen, K. *Inorg. Chem. Commun.* **2002**, *5*, 924–928.
- (62) Banerjee, S.; Drew, M. G. B.; Lu, C.-Z.; Tercero, J.; Diaz, C.; Ghosh, A. *Eur. J. Inorg. Chem.* **2005**, 2376–2383.
- (63) Yang, L.; Powell, D. R.; Houser, R. P. *Dalton Trans.* **2007**, 955–964.
- (64) Mukherjee, P.; Biswas, C.; Drew, M. G. B.; Ghosh, A. *Polyhedron* **2007**, *26*, 3121–3128.
- (65) Seth, P.; Das, L. K.; Drew, M. G. B.; Ghosh, A. *Eur. J. Inorg. Chem.* **2012**, 2232–2242.
- (66) Adams, H.; Clunas, S.; Fenton, D. E.; Gregson, T. J.; McHugh, P. E.; Spey, S. E. *Inorg. Chim. Acta* **2003**, *346*, 239–247.
- (67) Banerjee, S.; Chen, J.; Lu, C. *Polyhedron* **2007**, *26*, 686–694.
- (68) Adams, H.; Fenton, D. E.; Cummings, L. R.; McHugh, P. E.; Ohba, M.; Okawa, H.; Sakiyama, H.; Shiga, T. *Inorg. Chim. Acta* **2004**, *357*, 3648–3656.
- (69) Adams, H.; Clunas, S.; Fenton, D. E.; Gregson, T. J.; McHugh, P. E.; Spey, S. E. *Inorg. Chem. Commun.* **2002**, *5*, 211–214.
- (70) Chattopadhyay, S.; Bocelli, G.; Musatti, A.; Ghosh, A. *Inorg. Chem. Commun.* **2006**, *9*, 1053–1057.
- (71) Li, G.; Fang, H.; Cai, Y.; Zhou, Z.; Thallapally, P. K.; Tian, J. *Inorg. Chem.* **2010**, *49*, 7241–7243.
- (72) Chakraborty, J.; Thakurta, S.; Samanta, B.; Ray, A.; Pilet, G.; Batten, S. R.; Jensen, P.; Mitra, S. *Polyhedron* **2007**, *26*, 5139–5149.
- (73) Adams, H.; Clunas, S.; Fenton, D. E.; Handley, G.; McHugh, P. E. *Inorg. Chem. Commun.* **2002**, *5*, 1044–1047.
- (74) Guo, W.; Chen, X.; Du, M.; Escuer, A. *Inorg. Chem. Commun.* **2012**, *20*, 184–187.
- (75) Yildirim, L. T.; Kurtaran, R.; Namli, H.; Azaz, A. D.; Atakol, O. *Polyhedron* **2007**, *26*, 4187–4194.
- (76) Zhou, X.; Fang, H.; Ge, Y.; Zhou, Z.; Gu, Z.; Gong, X.; Zhao, G.; Zhan, Q.; Zeng, R.; Cai, Y. *Cryst. Growth Des.* **2010**, *10*, 4014–4022.
- (77) Addison, A. W.; Rao, T. N.; Reedijk, J.; Van Rijn, J.; Verschoor, G. C. *J. Chem. Soc., Dalton Trans.* **1984**, 1349–1356.